J|A|C|S
ARTICLES
Published on Web 11/20/2003

Colloidal Crystal Films: Advances in Universality and Perfection

Sean Wong, Vladimir Kitaev, and Geoffrey A. Ozin*

Contribution from the Materials Chemistry Research Group, Chemistry Department, 80 St. George Street, University of Toronto, Toronto, Ontario, Canada M5S 3H6

Received August 18, 2003; E-mail: gozin@chem.utoronto.ca

Abstract: For three-dimensional photonic crystals, made either by top-down microfabrication or by bottom-up self-assembly approaches, to comply with the stringent requirements of optical telecommunication applications, their degree of structural perfection and optical quality must meet an exceptionally high standard. Only with such superior quality photonic crystals can their unique optical properties be harnessed in optical devices and circuits constructed from micrometer-sized optical components. In this paper, we present a new strategy for making silica colloidal crystal films with a sufficiently high level of structural perfection and optical quality to make it competitive as a practical route to photonic crystal optical components. The attainment of this goal takes due cognizance of three key synergistic factors in the film formation process. The first recognizes the necessity to prepare high-quality silica spheres, which are highly monodisperse, with a polydispersity index significantly better than 2%, and the second recognizes that the population of spheres must be devoid of even the smallest fraction of substantially smaller or larger spheres or sphere doublets. The latter turns out to have a minimal effect on the polydispersity index, and yet a major detrimental effect on the overall structural order of the film. The third concerns the film-forming method itself, which necessitated the development of a novel process founded upon isothermal heating evaporation-induced self-assembly (IHEISA) of spheres on a planar substrate. This new method has several advantages over previously reported ones. It is able to deposit very high-quality silica colloidal crystal film rapidly over large areas, with a controlled thickness and without any restrictions on sphere sizes.

Introduction

Since Yablonovich and John theoretically showed the ability of 3-D periodic dielectric materials to possess a photonic band gap (PBG) in 1987,[1,2] PBG materials have become an important and popular area of research. The strong interest in PBG materials stems from their potential to confine and control the propagation of light with minimal losses. PBG materials are promising for many research areas that deal with electromagnetic radiation in the visible, UV, and near-infrared, while their low-loss wave-guiding properties are especially coveted by the telecommunications industry and touted to become new switching and wave-guiding materials of the future.

Many approaches have been proposed to fabricate 3-D periodically modulated dielectric materials, including nanomachining and photolithography[3,4] and 3-D holography.[5,6] While lithographic and holographic methods are undoubtedly promising, they are yet to overcome the challenge of producing very uniform submicrometer features consistently over large areas.[4] At the same time, self-assembly of colloidal spheres into opaline crystalline arrays offers a facile way to produce photonic crystals from well-defined building blocks.[7−9] Well-established procedures of preparation of inverse opals using diverse materials compositions[10,11] extend the versatility of the self-assembly approach. The self-assembly building blocks (typically silica or latex spheres) can be obtained with well-defined sizes and a very narrow size distribution, and therefore, the main challenge is to organize these spherical building blocks into ordered structures with minimal imperfection.

Compared to earlier methods of colloidal crystal formation using sedimentation, it has been found that vertical deposition utilizing evaporation-induced self-assembly driven by capillary forces[12] produces superior quality colloidal crystals, which have less defects and are not polycrystalline due to directional crystallization in the meniscus. In a procedure developed by Jiang and Colvin,[12] silica sphere dispersions are left to evaporate naturally to deposit high-quality thin colloidal crystal films on

(1) Yablonovitch, E. *Phys. Rev. Lett*. **1987**, *58*, 2059.
(2) John, S. *Phys. Rev. Lett.* **1987**, *58*, 2486.
(3) Fleming, J. G.; Lin, S.-Y. *Opt. Lett.* **1999**, *24*, 49.
(4) Divliansky, I.; Mayer, T. S.; Holliday, K. S.; Crespi, V. H. *Appl. Phys. Lett*. **2003**, *82*, 1667.
(5) Miklyaev, Y. V.; Meisel, D. C.; Blanco, A.; von Freymann, G.; Busch, K.; Koch, W.; Enkrich, C.; Deubel, M.; Wegener, M. *Appl. Phys. Lett*. **2003**, *82*, 1284.
(6) Campbell, M.; Sharp, D. N.; Harrison, M. T.; Denning, R. G.; Turberfield, A. J. *Nature* **2000**, *404*, 53.
(7) Garcia-Santamaria, F.; Salgueirino-Maceira, V.; Lopez, C.; Liz-Marzan, L. M. *Langmuir* **2002**, *18*, 4519.
(8) Gu, Z. Z.; Fujishima, A.; Sato, O. *Chem. Mater*. **2002**, *14*, 760.
(9) Blanco, A.; Chomski, E.; Grabtchak, S.; Ibisate, M.; John, S.; Leonard, S. W.; Lopez, C.; Meseguer, F.; Miguez, H.; Mondia, J. P.; Ozin, G. A.; Toader, O.; van Driel, H. M. *Nature* **2000**, *405*, 437.
(10) Stein, A.; Schroden, R. C. *Curr. Opin. Solid State Mater. Sci*. **2001**, *5*, 553.
(11) Meseguer, F.; Blanco, A.; Miguez, H.; Garcia-Santamaria, F.; Ibisate, M.; Lopez, C. *Colloids Surf*. **2002**, *202*, 281.
(12) Jiang, P.; Bertone, J. F.; Hwang, K. S.; Colvin, V. L. *Chem. Mater*. **1999**, *11*, 2132.

a vertically held substrate by the meniscus of an evaporating solvent. Naturally, this approach has two limitations: first, the long time of evaporation and second, more crucial, deposition is limited to smaller colloidal spheres that sediment slower than the solvent evaporates. The typical evaporation rate used by Jiang and Colvin[12] was ca. 10^{-3} cm^3/min, and sedimentation of dense (ca. 2.0 g/cm^3) silica effectively precludes formation of continuous large-area colloidal crystal films out of silica spheres larger than ca. 500 nm. Sedimenting colloidal spheres depart from the meniscus, and the deposition process is terminated.

Two principal approaches were proposed for keeping sedimenting large silica spheres suspended in the dispersion during the deposition process: mechanical agitation[13] and convection induced by a temperature gradient.[14] Mechanical agitation utilizing controlled gentle stirring was utilized successfully by Ozin and co-workers for confined crystallization of large silica spheres within controlled geometry surface relief patterns in optical microchips.[13,15] Mechanical agitation did not work well for the preparation of continuous colloidal crystal films. It seems that the swirl created by stirring disturbs the meniscus and impedes successful growth of continuous colloidal arrays. In another approach developed by Ozin's group, low pressure was used to accelerate ethanol evaporation and to counteract sedimentation.[16] This method proves to be very successful for self-assembling large (up to 1.5 μm) polystyrene latex spheres,[16] and while it extends the self-assembly range for the silica spheres up to ca. 800 nm diameter, counteracting the sedimentation rate of faster sedimenting silica colloids of ca. 1 μm in size seems to be quite challenging.

In another important development, Norris et al. reported the successful application of heating from the bottom of a vial containing a silica sphere dispersion in ethanol to induce convective flows and produce colloidal crystal films from 855 nm spheres.[14] While demonstrating the preparation of very high-quality films out of large silica spheres, this procedure proved to be difficult to reproduce. Several other groups have reported heating of sphere dispersions with some success.[17−19] The current consensus is[19] that there is no universally reliable and reproducible method for producing high-quality colloidal crystal film out of large silica spheres; however, there is a pressing need to develop a method useful for the routine production of high structural and optical quality crystalline sphere arrays to meet the challenge of demonstrating practical photonic crystal-based optical devices for telecommunications and other challenging applications that require operation in the near-infrared around 1.5 μm.

Herein, we describe a new procedure that we refer to as isothermal heating evaporation-induced self-assembly (IHEISA) as a fast universally reliable and reproducible method to produce well-ordered colloidal crystal films without any limitations imposed by silica sphere size. By heating the solvent (ethanol) very close to the boiling point, we are able to keep spheres suspended in the dispersion by convection flows, and the time of growth is shortened considerably to about 1 h for centimeter extents of the film. Below we discuss in detail what factors are important to achieve the highest quality colloidal crystal film in terms of both structural order and optical properties.

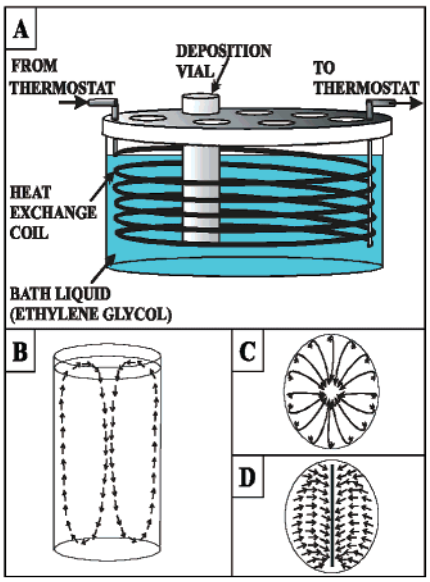

Figure 1. (A) Schematic of the isothermal bath setup for IHEISA deposition of colloidal crystal films. (B−D) Representation of convection patterns in a vial immersed into the IHEISA bath. (B) Side view. (C) Top view. (D) Top view when a glass slide is inserted in the center of the vial.

Experimental Section

Silica Particle Synthesis. Tetraethyl orthosilicate (TEOS) (Aldrich, 98%), tetramethyl orthosilicate (TMOS) (Aldrich, 99+%), ammonium hydroxide (Caledon Laboratories Ltd, 28−30 wt %, trace metal grade), water (Millipore), and anhydrous ethanol (Aldrich) were used as received. Monodisperse silica spheres with the sizes ranging from 200 to 1600 nm were produced using a modified Stöber procedure involving regrowth described by Giesche.[20] To produce silica spheres with low polydispersity of below 2%, the starting seed size used for regrowth was chosen to be at least four times smaller than the final sphere size aimed for. The silica spheres produced were cleaned by consecutive centrifuging, decanting, and redispersing, first in water (three times) and then in ethanol (three times). For several batches, removal of the doublets and smaller spheres (secondary seeds) were performed by fractionation using sedimentation in a column and removing the upper and the lower fractions several times. The size, shape, and polydispersity of the spheres were checked using a field emission scanning electron microscope (FE-SEM) (Hitachi S-4500).

Self-Assembly of Silica Spheres. Silica sphere dispersions (6−10 mL) with typical concentrations ranging from 5.5 to 25 wt % were placed in a cylindrical Opticlear glass vial (Fisherbrand, 3DR, Fisher Scientific). The vial with the sphere dispersion was immersed in an isothermal deposition chamber, which was machined from a solid block of high-density polyethylene (see Figure 1A) and heated to 79.8 ± 0.3 °C.

The chamber was filled with ethylene glycol and contained a heat exchange coil made out of copper tubing and connected to a recirculating heating bath (Isotemp 3016, Fisher Scientific). A tightly fit lid of the chamber had openings to fit the vials. The chamber was placed on a vibration damping rubber support (Fisher Scientific) resting on a sturdy table.

(13) Yang, S. M.; Miguez, H.; Ozin, G. A. *Adv. Funct. Mater*. **2002**, *12*, 425.
(14) Vlasov, Yu. A.; Bo, X.-Z.; Strum, J. C.; Norris, D. J. *Nature* **2001**, *414*, 289.
(15) Miguez, H.; Yang, S. M.; Ozin, G. A. *Appl. Phys. Lett*. **2002**, *81*, 2493.
(16) Kitaev, V.; Ozin, G. A. *Adv. Mater*. **2003**, *15*, 75.
(17) Ye, Y.-H.; LeBlanc, F.; Hache, A.; Truong, V. *Appl. Phys. Lett*. **2001**, *78*, 52.
(18) Goldenberg, L. M.; Wagner, J.; Stumpe, J.; Paulke, B. R.; Gornitz, E. *Langmuir* **2002**, *18*, 3319.
(19) Garcia-Santamaria, F.; Ibisate, M.; Rodriguez, I.; Meseguer, F.; Lopez, C. *Adv. Mater*. **2003**, *15*, 788.
(20) Giesche, H. *J. Eur. Ceram. Soc.* **1994**, *14*, 205.

Glass microscope slides (Corning, #2947) were cleaved in two pieces lengthwise, cleaned in freshly prepared Piranha solution (H_2SO_4/H_2O_2, 2:1), and rinsed copiously first with water and then with ethanol. To deposit a colloidal crystal film, the glass slides were carefully centered in a vial with the heated silica dispersion using either two small paper clips or a holder made out of the vial cup. After the glass slides were positioned in the vials, the chamber was covered with a crystallizing dish in such a way that evaporated ethanol could escape but depositing films would be subjected to minimal air current fluctuations. Typically, ethanol was completely evaporated from the dispersion, leaving a shiny, continuous colloidal crystal film on both the glass slide and the vial walls.

Characterization of the Opal Films. The microscopic quality of the colloidal crystal films, both top views and cross sections, was investigated using FE-SEM. For cross-sectional analysis, glass slides were carefully snapped to pieces with the help of a glasscutter. To produce better quality cross sections, colloidal crystals were lightly sintered by being fumed in TMOS vapors for several minutes and then being exposed to ammonia vapors. Low accelerating voltage of 1 to 2 kV was used for FE-SEM imaging of colloidal crystal films in order not to use any conductive coatings. The optical quality of the colloidal crystals was monitored using an UV−vis spectrometer with near-IR capabilities (Perkin-Elmer Lambda 900) in a transmission mode using a 1 to 2 mm aperture. An assessment of the colloidal crystal films quality over larger areas was made using an optical microscope (Olympus BX41).

Results and Discussion

First, we present a detailed description of IHEISA and discuss its advantages. Figure 1A displays a schematic of the heating bath in which a vial with a suspension of silica spheres is kept totally immersed, hence the term "*isothermal heating*". The bath is heated at 79.8 °C, slightly above the boiling point of ethanol, which evaporates fast and leaves a deposited colloidal crystal film on a vertically held glass slide inserted into the vial as described in more details in the Experimental Section.

The central idea behind the isothermal heating method is to circumvent sedimentation of large silica spheres during evaporation-induced self-assembly but not to adversely affect the meniscus. Two plausible scenarios of keeping spheres suspended by enhanced evaporation can be thought of: first, sustaining the ethanol evaporation rate faster than sedimentation and maintaining spheres in the meniscus of an evaporated dispersion, and second, inducing convection flows to keep the spheres in the dispersion. The sedimentation rate of silica spheres with the sizes ranging from 850 nm to 1 μm in ethanol is ca. 1.5−2.0 mm/h, and ethanol can be evaporated much faster than this (typically at least up to 1.5 cm/h). Yet, we always observed strong well-defined convection flows induced by ethanol evaporation. Even when ethanol evaporation is accelerated by low pressure,[16] the convection flows are also inevitably induced. We could image the convection patterns by either observing redispersion of a freshly sedimented silica sphere suspension upon placing the vial in the heating chamber or imaging fluffy gelatinous sol−gel aggregates (e.g., formed by hydrolysis of zirconium(IV) butoxide in ethanol containing minor amounts of water). The convection pattern induced by isothermal heating of ethanol suspension in a cylindrical vial is illustrated in Figure 1B,C. Liquid flows ascend near the walls of the vial and descend near the center, preserving the cylindrical symmetry of the vial in the absence of a glass slide. When the glass slide is inserted in the center of the vial, the cylindrical symmetry is broken, but the flow pattern is largely preserved,[21] as shown in Figure 1D. A similar convection pattern is observed for a solvent evaporating out of a cylindrical vial at low pressures. In addition, there is no visible convection in a hermetically closed vial inserted in a hot bath. *Thus, we can conclude that IHEISA convection is predominantly of the Bénard−Marangoni type driven by surface cooling of the evaporating liquid.*[22−24] *This type of convection pattern is clearly distinct from one induced by heating the vial from the bottom.*[14] The latter is the case of predominantly Raleigh−Bénard convection,[25] with some contribution of surface-induced effects due to liquid evaporation. What is important for colloidal sphere deposition is that the flow patterns of Raleigh−Bénard convection are much more dependent on the vial geometry, i.e., the aspect ratio, which changes upon liquid evaporation. As a result, for cylindrically shaped vials with a length-to-width ratio of 3.57;1, typically used in the vertical deposition, convection patterns induced from top to bottom are not stable. Hence, it is quite difficult to control the deposition process and its reproducibility, as noted in the literature.[19] In IHEISA we implemented heating of the vial totally immersed in a heating chamber to induce the convection patterns, which are stable, much easier to sustain,[22] and very importantly, invariant upon ethanol evaporation from the sphere dispersion. The latter is crucial for the production of uniform large-area high-quality colloidal crystal films.

We have tested several solvents other than ethanol (methanol, 2-propanol, water) and their mixtures for their use in IHEISA and found ethanol to be the best choice. Methanol works as well as ethanol, but it is clearly less preferable to evaporate due to its toxicity. Dispersions in 2-propanol and 2-propanol−ethanol mixtures yield substantially thinner films compared to the dispersions in pure ethanol with the same concentrations. Films produced from water dispersions show vertical stripes of alternating thinner and thicker films presumably due to the better wettability of the glass substrate with water, which favors fluctuations in the meniscus and uneven deposition. We have also experimented with different sizes and shapes of vials to produce colloidal crystal films of greater width than our commonly used 1.25 cm substrates. We found that cylindrically shaped vials work the best since the convection patterns there are isotropic and the best defined. We could easily produce films at least 2.5 cm wide using larger cylindrical vials. To produce larger area films, the major impediment is the large amount of sphere dispersion required to fill the deposition vial. We also found that rectangular-shaped vials work satisfactorily, which allows for the more economic (with respect to the volume of sphere dispersions used) production of arbitrary large areas, and should be of importance for future technological use of large-area colloidal crystal films.

Despite the apparent simplicity of the isothermal heating, it proved to be quite a formidable challenge to produce the highest quality films that we aimed at. The optimal range of parameters for IHEISA happens to be quite narrow. Well-ordered uniform silica colloidal crystal films were formed only when the temperature in the deposition vial remained in the range between 79.5 and 80.2 °C. Higher temperatures caused ethanol to boil

(21) Cerisier, P.; Perez-Garcia, C.; Jamond, C.; Pantaloni, P. *Phys. Lett.* **1985**, *112A*, 366.
(22) Koschmieder, E. L.; Prahl, S. A. *J. Fluid Mech.* **1990**, *215*, 571.
(23) Rosenblat, S.; Davis, S. H.; Homsy, G. M. *J. Fluid Mech.* **1982**, *120*, 91.
(24) Wagner, C.; Friedrich, R.; Narayanan, R. *Phys. Fluids* **1994**, *6*, 4.
(25) Pasquetti, P.; Ceriser, P.; Le Niliot, C. *Phys. Fluids* **2002**, *14*, 277.

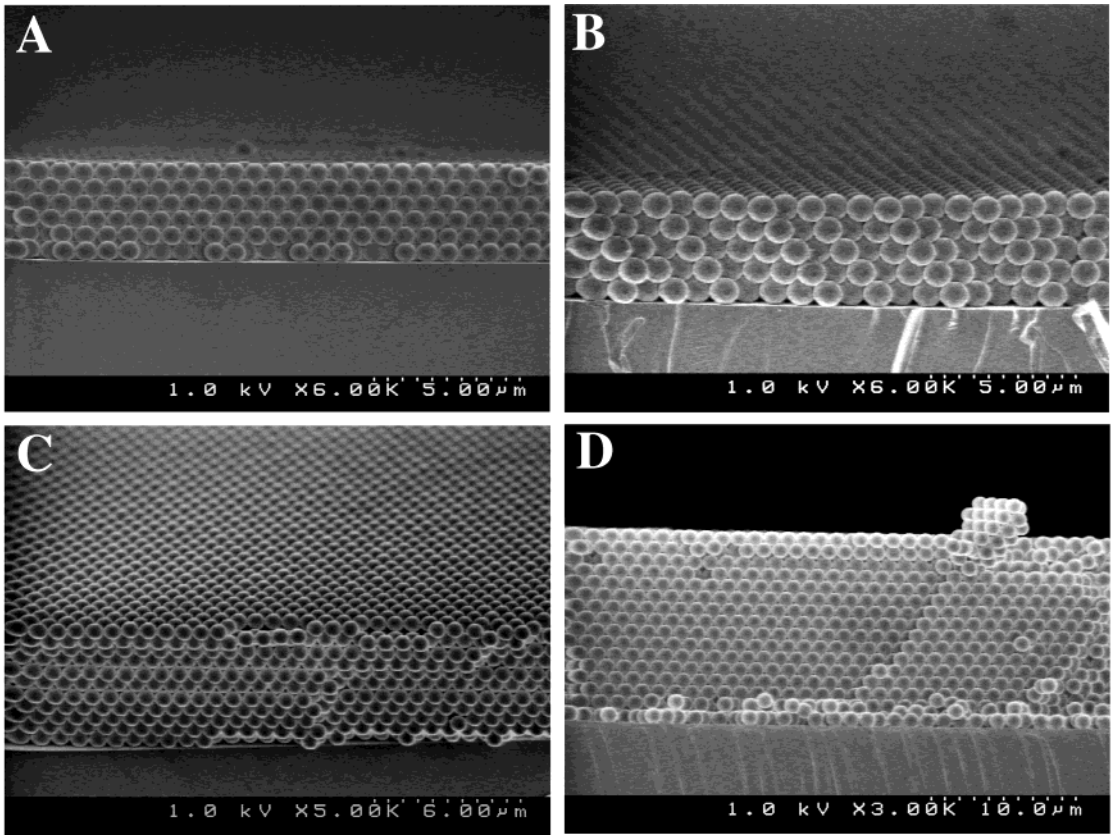

Figure 2. Representative SEM images of the cross sections of the silica colloidal crystal films produced by IHEISA using (A) and (C) 635 nm, (B) 850 nm, and (D) 1.0 μm spheres.

and led to irregular colloidal crystal films. At lower temperatures, films became thin and disordered. Moreover, film deposition only occurred when the level of the ethanol was below the level of liquid in the heating apparatus. In the optimized procedure, we typically started with the level of the dispersion in the vial about 0.5 cm higher than the level of the heating liquid in the bath to allow temperature equilibration of the dispersion (about 5 min for our setup) before the actual deposition takes place. The temperature in the bath during the deposition should not fluctuate more than ca. 0.05 °C. Silica colloidal crystal films produced under such optimized conditions show a high degree of order, as seen by inspection of Figures 2 and 3. In addition, the supplementary Figure S1 presents color photographs of several silica colloidal crystal films deposited on a half-cut glass slide. Clearly, photographs cannot capture all of the opalescent beauty, but the quality and the uniformity of the samples can be appreciated.

Figure 2 shows cross-sectional FE-SEM images of the colloidal crystal films formed by 635 nm, 850 nm, and 1.0 μm silica spheres. The long-range vertical ordering and virtual absence of defects is apparent. Different film thicknesses can be obtained as demonstrated in Figure 2. It will be discussed later that 5−10 sphere layer films are typically produced at sphere concentrations of 4−7 wt % most commonly used in our experiments. It can be seen, especially for thicker films, that the top surface is most indicative of the order in the colloidal crystals, since the majority of the defects originating in the lower layers inevitably propagate to the top.

The top view images of the (111) plane of silica colloidal crystal film produced from 480, 635, 850, and 1000 nm silica spheres using IHEISA are shown in Figure 3. These pictures clearly demonstrate the degree of perfection in colloidal crystal order achievable with the isothermal evaporation of highly monodisperse silica sphere dispersions. For the high-quality films we have obtained, perfect domain size ranges routinely in the range of 100 × 100 spheres. Imaginary lines connecting the centers of sphere planes in Figure 3 run perfectly straight, corroborating the high level of domain order.

The high degree of order of the colloidal crystal films produced with IHEISA is preserved over large areas, as can be judged by the optical spectra shown in Figure 4. These spectra were taken using a UV−vis−NIR spectrophotometer in transmission mode and are presented in Figure 4 without any smoothening or correction for background or scattering. Discernible discontinuities in the spectra at around 850 nm are caused by a detector change of the spectrometer. Both Fabry−Perót fringes and higher energy optical flat bands can be clearly observed. Fabry−Perót fringes originate from the finite film thickness and indicate the uniformity of film thickness over large areas.[26] The characteristic structure of the higher energy bands is clearly seen. The main physical reason that we could clearly observe well-resolved higher energy bands[27] for all the spectra shown in Figure 4 is due to a decrease in scattering of the samples originating from the perfection in colloidal crystal order in the film.

Figure 4 displays the variation of the spectra with the change in silica sphere size. Both stop bands and higher energy flat

(26) Bertone, J. F.; Jiang, P.; Hwang, K. S.; Mittleman, D. M.; Colvin, V. L. *Phys. Rev. Lett.* **1999**, *83*, 300.
(27) Miguez, H.; Kitaev, V.; Ozin, G. A. *Appl. Phys. Lett*, submitted for publication, 2003.

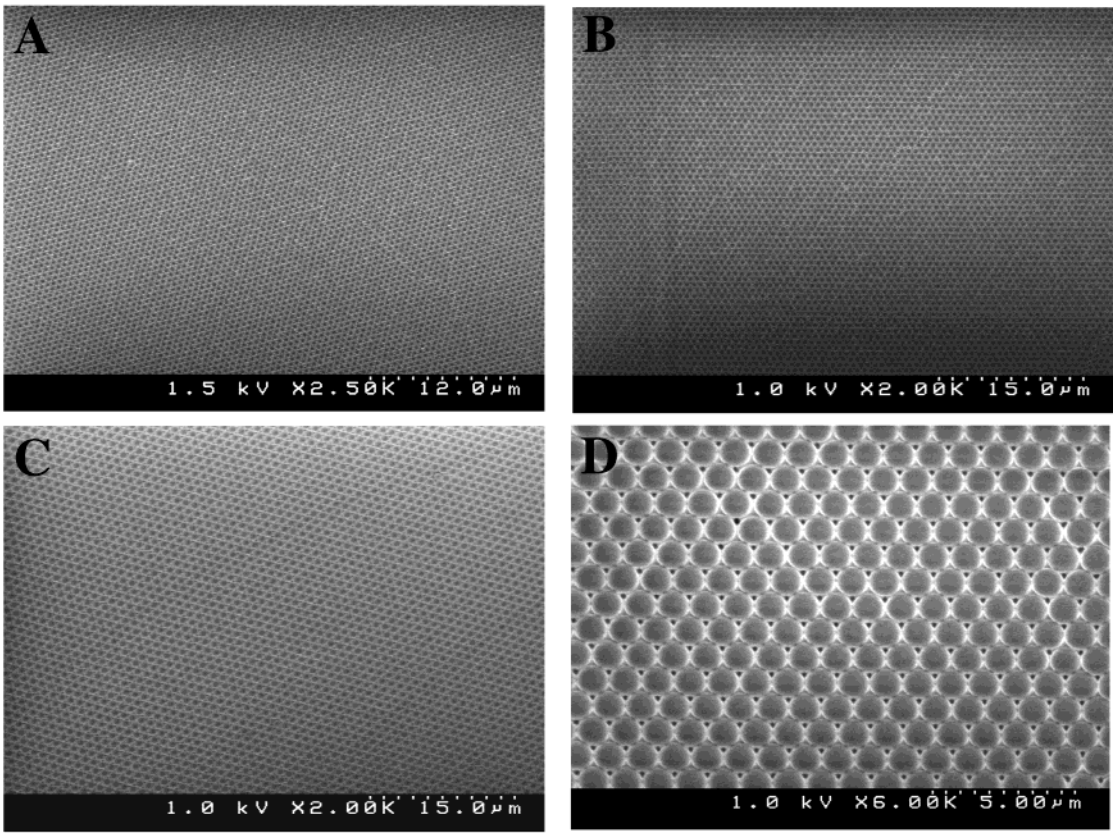

Figure 3. SEM images of a top view of the silica colloidal crystal films demonstrating the high degree of long-range ordering achievable with IHEISA. (A) 480 nm, (B) 635 nm, (C) 850 nm, and (D) 1.0 μm.

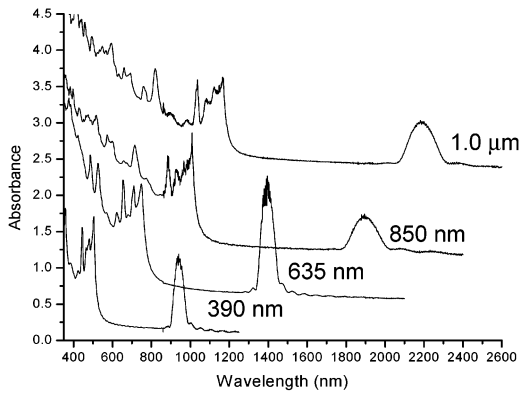

Figure 4. UV−vis−NIR spectra of the colloidal crystal films composed of 390 nm, 635 nm, 850 nm, and 1.0 μm silica spheres. Spectra are shifted along the *y*-axis for presentation clarity. Note the very well-resolved higher energy flat bands and Fabry−Perót fringes.

bands are red-shifting for larger spheres packing with larger lattice constants, as expected. The larger the spheres, the broader the spectral range available for optical studies, and more higher energy bands can be experimentally observed. In general, the peak positions of the spectra follow the scaling law for photonic crystals, i.e., the shape of the spectra remains the same while the wavelength corresponding to both the stop band and higher bands increase with the sphere diameter. For 1.0 μm silica spheres (Figure 4, the top spectrum), the stop band lies at ca. 2180 nm. Thus, with IHEISA one can easily prepare colloidal crystal films serving as photonic crystals in a wide spectral range from the visible to the near-IR. We have not systematically studied deposition of silica spheres larger than 1 μm, since we feel that it is not advantageous for self-assembly to compete with modern lithographic methods when the feature size becomes larger than a micrometer. At the same time, for producing optical devices having submicrometer features, self-assembly should remain competitive with, and complementary to, micropatterning techniques.

Since we have been able to easily obtain highly ordered silica colloidal crystal films, we have systematically investigated the relationship between the microscopic order and optical properties of the colloidal crystals using SEM and UV−vis−NIR spectroscopy, respectively. The key finding of this study is that the highest structural quality of the colloidal crystal films observed by SEM is always translated to the highest quality optical spectra for the samples of more than five layers thick. The reverse is not always true, as can be seen in Figures 5 and 6, which show the UV−vis−NIR spectrum and SEM images of the same colloidal crystal film formed by 410 nm silica spheres. While the quality of the optical spectrum shown in Figure 5 can be hardly distinguished from the best spectra we have obtained, the SEM reveals an appreciable number of line dislocations and microcracks. These observations suggest two conclusions. The first is that SEM is the best and most revealing method for evaluation of colloidal crystal perfection, which is certainly not surprising. The second is that the optical properties of colloidal crystals are indeed quite tolerant to dislocation defects and stacking faults, as previously found experimentally[28] and confirmed theoretically.[29] Such findings open the possibility that

(28) Vlasov, Yu. A.; Astratov, V. N.; Baryshev, A. V.; Kaplyanskii, A. A.; Karimov, O. Z.; Limonov, M. F. *Phys. Rev. E* **2000**, *61*, 5784.
(29) Wang, Z. L.; Chan, C. T.; Zhang, W. Y.; Chen, Z.; Ming, N. B.; Sheng, P. *Phys. Rev. E*, **2003**, *67*, 016612.

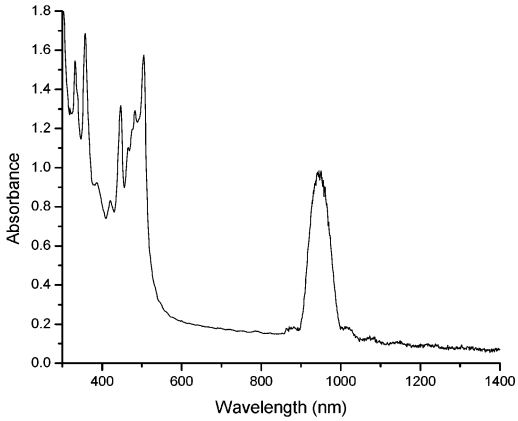

Figure 5. UV−vis−NIR spectrum of the silica colloidal crystal film formed by 410 nm spheres.

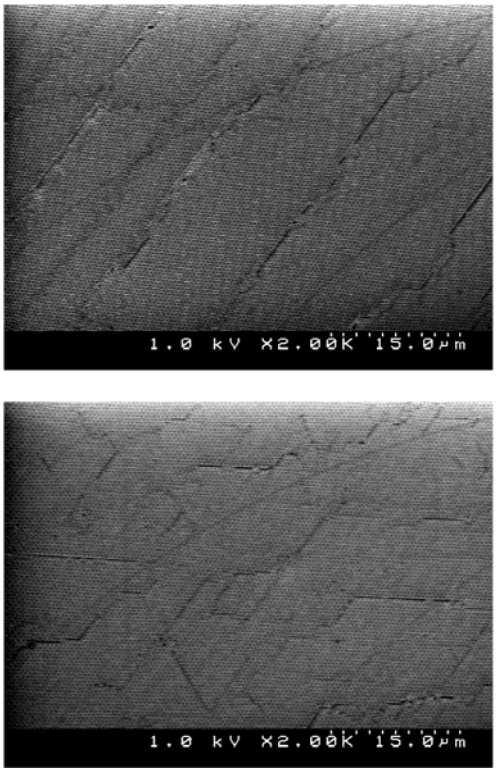

Figure 6. Two representative top view SEM images of colloidal crystal films formed by 410 nm silica spheres, which were used to obtain the spectrum shown in Figure 5.

self-assembly of colloidal spheres might be successfully implemented in practical 3-D photonic devices.

One quite interesting observation is that well-defined higher energy flat bands can be clearly observed for relatively thin films (as thin as ca. five layers for 850 nm silica spheres and larger), for which attenuation of the stop band remains quite low at several dB (see for example Figure 4 or 7). The attenuation of the higher bands is always appreciably higher than that of the stop band. Thus, highly ordered silica colloidal crystal films comprised of a limited number of layers may be useful for compact 3-D photonic crystal devices utilizing higher energy optical flat bands. Figure 7 displays UV−vis−NIR spectra of four samples of 635 nm silica colloidal crystal films deposited by IHEISA using dispersions with different silica concentrations.

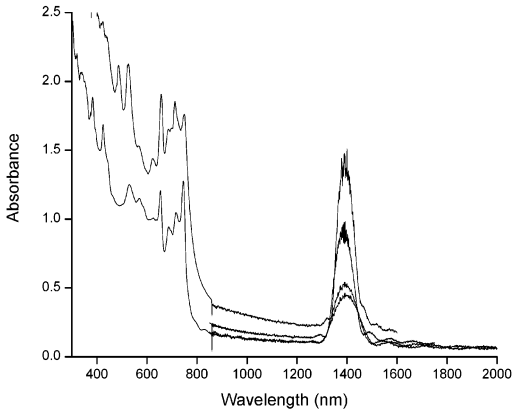

Figure 7. UV−vis−NIR spectra of 635 nm silica colloidal crystal films produced using different sphere dispersion concentrations of 7, 10, 13, and 24 wt % (from bottom to top spectra). High-energy flat bands are shown only for the top and bottom spectra for clarity of presentation.

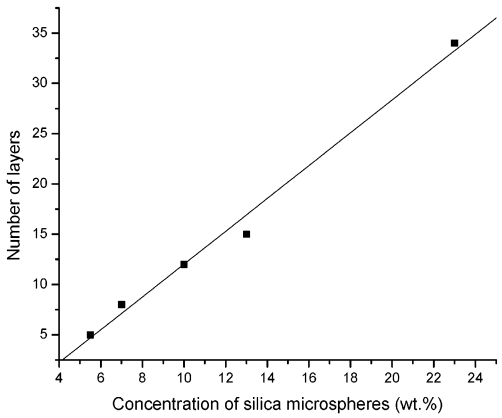

Figure 8. Dependence of the thickness of the colloidal crystal films formed using IHEISA upon concentration of 635 nm silica spheres in dispersion.

The increase in the attenuation of the stop band originates from an increase in efficiency of Bragg diffraction of light due to the larger number of lattice units present in thicker films formed at higher sphere concentrations. The thickness of the colloidal crystal films produced in a single deposition run by IHEISA ranged from a few layers to more than 30 layers and can be adjusted by varying the concentration of silica spheres. Figure 8 shows the dependence of the colloidal crystal film thickness (plotted as a number of layers) vs concentration of 635 nm silica spheres. The number of layers was averaged for three points taken horizontally (that is, perpendicular to the direction of the drying liquid front). In silica colloidal crystal films produced by IHEISA, we observed minimal or no gradients in the vertical direction, a problem which is inherent to evaporation-induced self-assembly because of the change in dispersion concentration upon solvent evaporation. We do, however, observe some variance in colloidal crystal film thickness between the inner and outer edges of the substrate. Typically, the film deposited onto the edges of the glass slide are 1 to 2 layers thicker compared to the central areas, which makes an appreciable difference for thin (5−10 layers) films, but less significant for the thicker films. We believe this difference originates from the distribution of convection flows (Figure 1B). The spheres are transported upward close to the walls of the vial, which should uplift the meniscus, increase the sphere concentration in the meniscus, and lead to thicker

deposited films at the edges of the substrate. On the other hand, in the center, the liquid flows are descending (see Figure 1B), which should both decrease the sphere concentration in the meniscus and suppress the drying zone of the meniscus,[12,30] causing formation of thinner colloidal crystal films.

It should be noted that to obtain thick colloidal crystal films, high-concentration silica sphere dispersions (up to 25 wt %) should be used. The thickness of the films produced by IHEISA is about a factor of 2 less than that reported by Jiang and Colvin for natural ethanol evaporation.[12] One of the factors responsible for such behavior can be the lower surface tension of ethanol near its boiling point, which translates into a thinner meniscus height. Another factor is that the rapid evaporation of overheated ethanol near the surface may occur faster than the physical transport of the spheres into the drying area. A related argument is that only the part of the meniscus that is thicker or comparable to the sphere diameter can participate in the film deposition. Colloidal spheres can hardly be transported into the thinner area of the meniscus, being effectively pinned down to the substrate. This argument may also explain an appreciable difference between the calculated height of the meniscus and the drying part of the meniscus, L, in the Nagayama model[30] reported by Jiang and Colvin.[12] For the larger spheres, the effective part of the meniscus that they can fit into is much smaller, which should lead to less colloidal deposition and thinner colloidal crystal films.

There are several approaches available to produce thicker colloidal crystal films. One, which was recently described by Park et al.,[31] involves tilting of the substrate. In IHEISA, we found it works only to a limited extent. By tilting the substrate, we are indeed able to produce thicker colloidal crystal films on one side of the slide. However, such films often become irregular, which we attribute to the distortion of the vertical convection cells by the tilted substrate. A simpler approach to increase the film thickness, which we found works very well with IHEISA, is multiple deposition. There, to ensure integrity of the previously deposited films in subsequent depositions (i.e., peeling off or partial redispersion), fuming with TMOS for several minutes at 80 °C was used to sinter the colloidal crystal film very lightly (the shift in the Bragg peak is almost undetectable at less than 5 nm). This treatment ensures 100% successful multiple depositions in IHEISA. In addition, by using multiple depositions we could easily obtain multilayer colloidal crystal films composed of different silica sphere sizes. Figure 9 exhibits several examples of such multilayers: AB (Figure 9A) formed by 850 and 260 nm silica spheres and ABA (Figure 9B) 850/480/850 nm composite colloidal crystal. The crystalline order of each layer shown in Figure 9 is well preserved after subsequent depositions. The universal capability of IHEISA for preparing colloidal crystal films out of any size silica spheres is nicely demonstrated by Figure 9. It should be mentioned that for silica spheres smaller than 300 nm, the order of the film decreases slightly, which can be due to two factors. First, smaller spheres are naturally more polydisperse, and second, very fast deposition may not be optimal for the arrangement of the small highly mobile colloidal spheres.

Thick multilayers (at least 30 μm and typically up to ca. 50 μm) composed of any silica sphere sizes can be obtained before delamination starts to pose a problem. By varying the silica sphere concentration, the thickness of the individual layers in the composite colloidal crystal films can be carefully controlled, and multilayer colloidal crystals can be prepared very efficiently using IHEISA.

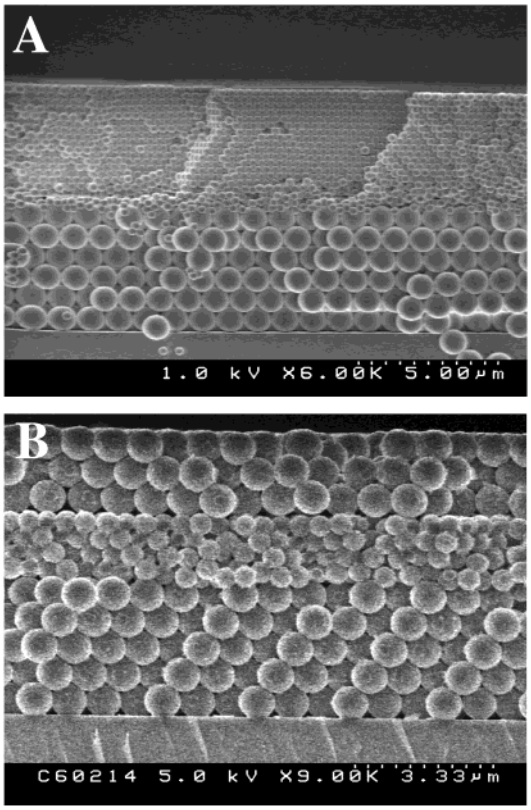

Figure 9. SEM images of cross sections of composite silica colloidal crystal films obtained by consecutive deposition using two different sphere sizes. (A) Two-layer colloidal crystal structure formed first using 850 nm and then 260 nm sphere layers on a glass substrate. (B) Three-layer composite colloidal crystal 850/480/850 nm on a glass substrate.

IHEISA also proved to be a versatile universal method capable of producing binary colloidal crystals shown in Figure 10. Figure 10A,B presents binary colloidal crystals formed by two types of spheres with a large diameter ratio,[16] specifically 850 nm silica and 150 nm polystyrene, both carrying a negative surface charge. Large spheres attain a high degree of FCC ordering with large domain sizes (typically 50 × 50 spheres), as can be seen in Figure 10A. The interstitial spaces are filled with well-ordered smaller spheres. Here, using IHESA, packing of large silica spheres could be easily achieved, which was more challenging to attain using a previously described low-pressure approach.[16] It can be clearly seen in Figure 10B that the small latex spheres are quite heavily necked together after ca. 2 h of film exposure at 80 °C used in IHEISA. This shows one of the few IHEISA limitations: polystyrene sphere arrays formed using this method are well-ordered but become heavily necked during deposition. At the same time, this offers a possibility of formation of silica arrays sintered in the interstices with smaller latex spheres, which has an important advantage of minimizing cracks in colloidal crystal films. Figure 10, parts C and D, presents AB_2 and related binary colloidal crystal films formed by 850 and 480 nm silica spheres. The ratio of these two sphere diameters is 0.57, which is close to ideal for AB_2 structures (0.58). The binary colloidal crystal film imaged in Figure 10,

(30) Dimitrov, A. S.; Nagayama, K. *Langmuir* **1996**, *12*, 1303.
(31) Im, S. H.; Kim, M. H.; Park, O. O. *Chem. Mater.* **2003**, *15*, 1797.

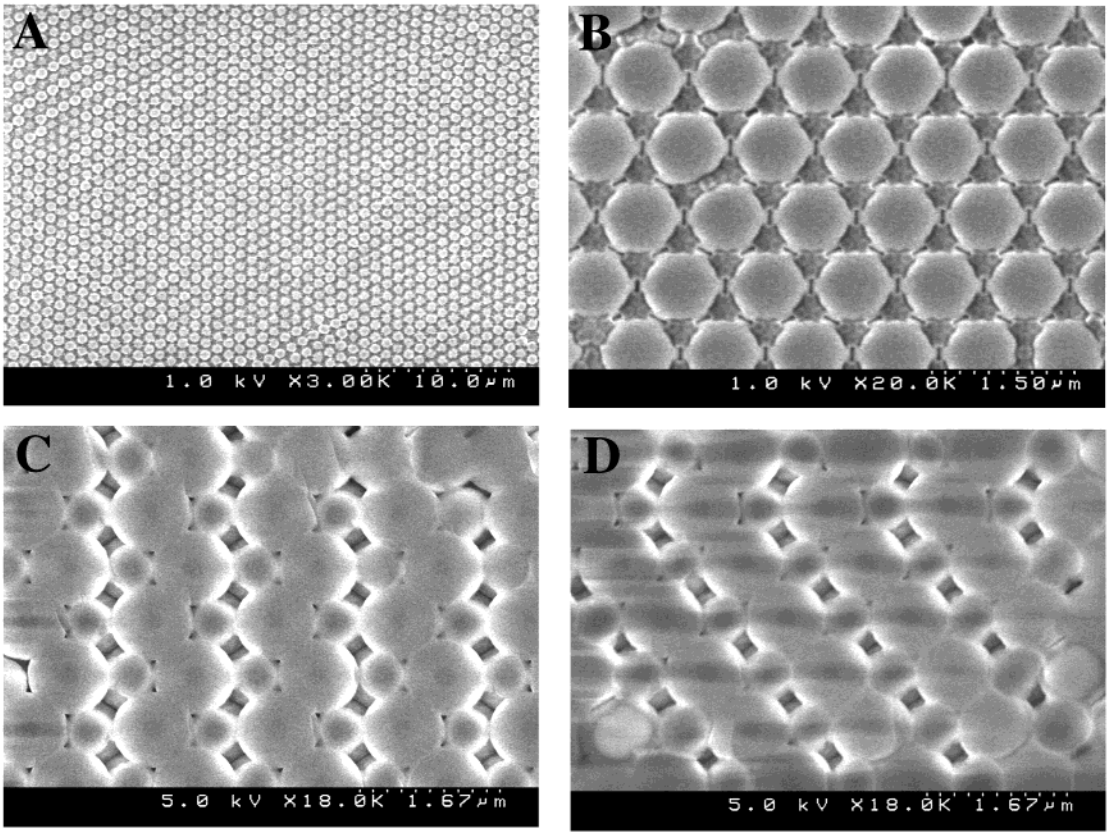

Figure 10. SEM images of binary opal films obtained by using IHEISA. (A) and (B) Top views of films formed by large 850 nm silica spheres and small 150 nm polystyrene latex spheres packed in interstices. (C) and (D) Cross-sections of AB_2 and AB_2-like packing obtained from 480 and 850 nm spheres.

parts C and D, was produced by the consecutive deposition of 850 nm spheres on top of the layer of 480 nm spheres, which was not necked with TMOS. The top layer of this film consists exclusively of 850 nm closely packed planes, while the cross section reveals an AB_2 binary sphere arrangement (Figure 10C) with persistent chevron-like defects (Figure 10D) associated with stacking irregularities (or random stacking) of closely packed planes formed by larger and smaller spheres. We are currently working to reproduce and further explore these interesting findings.

Defects in Silica Colloidal Crystal Films. The issue of structural perfection of colloidal crystal films closely relates to that of defects in colloidal crystal lattices and their origin, since the films prepared by IHEISA under optimal conditions do not contain any amorphous nonordered regions. Through detailed SEM analysis of IHEISA colloidal crystal films, we have identified two major causes of defect formation, namely, dislocations and microcracks, with the latter arising upon drying.

One of our crucial findings is that the dislocations can be directly linked to the quality of silica spheres used for the preparation of colloidal crystal films. The quality of the silica spheres should be considered as two closely related yet separate issues: the polydispersity of spheres and the presence of impurity spheres with sizes appreciably different from the average sphere size of the main batch. The polydispersity issue is historically given most attention. It is commonly accepted that the polydispersity of colloidal spheres should be better than 2% to minimize crystal imperfections required for demanding optical applications. Our observations confirm these findings. The high-quality colloidal crystal lattice with long-range order maintained for every sphere in an array shown in Figure 3 can be only achieved for a polydispersity lower than 2%. It should be pointed out that to measure reliably such low polydispersity is challenging. Scanning electron microscopy is the most commonly used direct method of measuring polydispersity since other methods, such as dynamic light scattering or related methods, can hardly be used for sedimenting large silica spheres. With the advanced Field Emission SEM Hitachi S-4500, which we used for our studies, the absolute error of measuring sphere size is ca. 5% (as specified by the manufacturer), while the relative error (e.g., for measuring the same sphere twice) should not exceed 2%.[32] We found it is difficult to measure sphere diameter reliably with a relative error much better than 2% even for larger 500−1000 nm spheres. The realistic error estimate found upon several repeated measurements is ca. 1.5%. Thus, it is quite hard to obtain reliable polydispersity values below 2%, especially considering that one has to measure several hundred spheres to collect a statistically meaningful sample size. For the several batches of silica spheres regrown from seeds at least 4 times smaller than the resulting spheres and with the starting polydispersity below 5%, the resulting polydispersity was measured to be at least 1.5% or better.

Let us now look in detail into the influence of impurity spheres on the order of the colloidal crystal films. We will distinguish three major types of undesirable impurities: spheres with appreciably larger and appreciably smaller diameters and doublets.

First, the larger spheres (other than doublets) are very rare in silica regrowth (can be only observed upon contamination

(32) Technical documentation of Hitachi S-4500 FE-SEM.

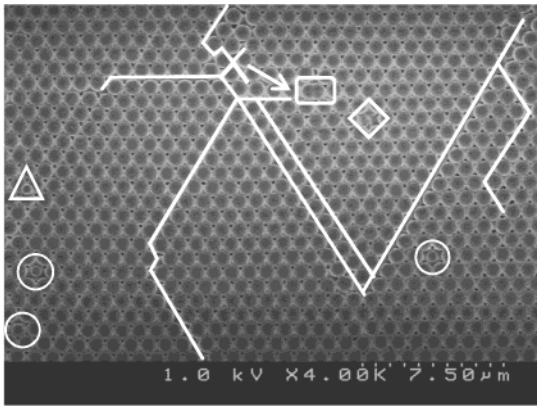

Figure 11. An SEM image of the top (111) plane of the colloidal crystal film conveniently demonstrating microscopic defects, which occur due to the presence of undesirable impurity particles with sizes different than the main silica sphere batch. White circles illustrate substitutional defects arising upon replacing the main batch spheres by smaller ones. The white triangle outlines a smaller sphere occupying an interstitial site. The white diamond points out a location of a missing sphere in the lattice. The white rounded rectangle demonstrates how doublet silica particles affect the colloidal crystal. White multiple lines highlight line dislocations and their long-range propagation in the colloidal crystal film.

of the seeds with larger spheres) and are not a major impurity factor in the case of silica colloidal crystal films considered in our work. Smaller spheres, on the other hand, can often be present, since they are secondary seeds formed during regrowth of silica. The doublets (dumbbell-shaped colloids) are the product of two spheres adhering together during silica regrowth and are also often seen.

Figure 11 presents an illustrative example of several types of defects caused by impurities in a top (111) plane of a colloidal crystal film cast out of nonpurified silica spheres. First, it can be seen that line dislocations (highlighted with white lines in Figure 11) are the most persistent defect type with the most detrimental influence on the order. These dislocations often extend over large distances, and they merge together to form the grain boundaries for crystalline domains. It can be clearly seen that one of the line dislocations originates from the presence of a doublet impurity (pointed out by the white rounded rectangle), causing lattice misalignment. Because of the propagation of dislocations, the presence of doublets (as well as any impurities of larger size) is very detrimental to the order in colloidal crystal films. Impurities with a smaller sphere size are either just substituting for large spheres in the lattice (shown by white circles) or occupying interstitial sites (shown by the white triangle). The latter is typically less common. The substitutional defects as well as missing spheres (outlined by the white diamond) are localized defects; hence, they do not affect the order in colloidal crystals as much as the dislocations. Smaller spheres packed in interstitial sites may seem "harmless" in a top layer, yet they most certainly cause misalignment of the neighboring crystalline planes and an associated propagating line defect.

Witnessing the unmistakable detrimental nature of impurity particles, it is instructive to understand how well the polydispersity can indicate impurities and, hence, the quality of the colloidal crystal films. Let us consider a hypothetical example of the batch of silica spheres with a size of 1.0 μm and polydispersity of 1.50%, to which we add a very small amount of larger 1.5 μm spheres, specifically 1 per every 1000 of the original spheres. It is easy to calculate that polydispersity will change negligibly from 1.50 to 1.55% (in fact, imperceptibly for most experimental measurements). In the "contaminated" batch, larger spheres inevitably create line defects, one per 1000 spheres. However, 1000 spheres is just the volume of $10 \times 10 \times 10$ spheres, which will be, in fact, an average domain size (if not smaller due to other factors) of the colloidal crystal films produced from this batch. In other words, the polydispersity may not be a very indicative predictive parameter for the order of the colloidal crystal films produced using spheres containing a minor amount of impurity particles with appreciably different sizes. Such a situation is very common for the spheres produced by regrowth. *All these arguments justify our findings that exhaustive purification of silica spheres even from the seemingly minor traces of impurity spheres is necessary for producing highest quality colloidal crystal films*.

The second dominant type of defects in colloidal crystal films is microcracks, which can be easily observed using an optical microscope at magnifications starting as low as 100×.

A typical size of a microcrack ranges from a fraction of to more than a sphere diameter. The microcracks are largely unavoidable for colloidal crystal films formed by pure silica spheres. Their underlying fundamental cause is drying of the water and alcohol solvation layer surrounding the silica spheres[33] after they self-assemble into a closely packed array from the dispersion. The loss of the solvation layer causes a decrease in an individual sphere size, forcing the closely packed array to shrink and give rise to cracks. Typical crack density is about one per hundred to several hundred spheres. Highest quality films have the smallest number of cracks, while the cracks are deeper. Since the solvation layer is not changing proportionally with the size of the spheres, silica colloidal crystals formed out of smaller spheres naturally exhibit more cracks.

Cracks do not appreciably affect the order parameter and optical properties measured for relatively large-area silica colloidal crystal films, since the portion of the surface occupied with cracks is minor (<1%) and they tend to average out. However, the cracks may pose a problem for miniature optical devices relying upon light interaction with small well-defined areas of colloidal crystals. A suitable approach to reduce cracks is to introduce some additives to prevent spheres from changing their size upon close packing into a colloidal crystal array. One possible way to implement this has already been mentioned in the discussion of binary colloidal crystals (Figure 10A,B). There, the addition of smaller PS latex spheres, which undergo necking during IHEISA and cement the silica colloidal crystal, eliminates cracking. Other polymer spheres compatible with silica dispersions can be used as well. We also explored another approach to minimize crack formation, where small amounts of TEOS or TMOS are added to the silica sphere dispersion in ethanol during IHEISA deposition to react with water physisorbed on the surface and to form an additional silica layer, thus preventing silica spheres from shrinkage. Our preliminary results indicate that this approach indeed minimizes the cracks, and we are currently investigating optimal conditions for this process.

Conclusions

We have demonstrated that the fast, reliable, and reproducible procedure of isothermal heating evaporation induced self-

(33) Miguez, H.; Tetreault, N.; Hatton, B.; Yang, S. M.; Perovic, D.; Ozin, G. A. *Chem. Commun.* **2002**, *22*, 2736.

assembly (IHEISA) enables production of highly ordered silica colloidal crystal films without any limitations imposed by the size of silica spheres. IHEISA employs precisely controlled uniform heating of the dispersion of silica spheres in a vial at 79.8 °C to induce convective flows intended to keep spheres suspended during vertical deposition in the meniscus. The capability of IHEISA to produce composite colloidal crystal multilayers and binary colloidal crystal films was demonstrated. We showed that the low polydispersity of the silica spheres plus minimization of impurity spheres are crucial requirements for producing the highest quality colloidal crystal films. Specifically, impurity spheres are responsible for initiation of line dislocations propagating in the colloidal crystals. Thus, such impurities are very detrimental even in extremely small amounts and have to be removed to produce colloidal crystal films having very low defect densities. For such highly ordered colloidal crystal films, very low background scattering and well-resolved higher order flat bands were observed in UV−vis−NIR spectra. Finally, by monitoring the quality of the colloidal crystal films both by scanning electron microscopy and optical spectroscopy, we have found that the optical quality, but not necessarily light scattering losses, is reasonably tolerant to defects in the colloidal crystals. All of this bodes well for the potential of IHEISA colloidal crystal films for use in practical optical devices.

Acknowledgment. G.A.O. is Government of Canada Research Chair in Materials Chemistry. He acknowledges the Natural Sciences Engineering Research Council of Canada and the University of Toronto for financial support of this work. We thank Ulrich Kamp for the help with the photography of colloidal crystal films.

Supporting Information Available: Three photographs showing the iridescence of high-quality opal films (PDF). This material is available free of charge via the Internet at http://pubs.acs.org.

JA0379969